J. Marine Sci. Appl. (2012) 11: 164-168
DOI: 10.1007/s11804-012-1118-1

The Calculations of Propeller Induced Velocity by RANS and Momentum Theory

Qiuxin Gao*, Wei Jin and Dracos Vassalos

Department of Naval Architecture and Marine Engineering, University of Strathclyde, Glasgow G4 0LZ, UK

Abstract: In order to provide instructions for the calculation of the propeller induced velocity in the study of the hull-propeller interaction using the body force approach, three methods were used to calculate the propeller induced velocity: 1) Reynolds-Averaged Navier-Stokes (RANS) simulation of the self-propulsion test, 2) RANS simulation of the propeller open water test, and 3) momentum theory of the propeller. The results from the first two methods were validated against experimental data to assess the accuracy of the computed flow field. The thrust identity method was adopted to obtain the advance velocity, which was then used to derive the propeller induced velocity from the total velocity field. The results computed by the first two approaches were close, while those from the momentum theory were significantly overestimated. The presented results could prove to be useful for further calculations of self-propulsion using the body force approach.
Keywords: propeller induced velocity; RANS; momentum theory; self-propulsion
Article ID: 1671-9433(2012)02-0164-05

1 Introduction

Model tests of ship self-propulsion were traditionally the only way to evaluate the powering performance and the propeller design of a ship. With the rapid advances in the field of computational fluid dynamics (CFD) and high performance computing (HPC), numerical simulations of ship self-propulsion have recently gained increasing attention.

There are two methods to model propellers in the study of hull-propeller interaction or ship self-propulsion. One is the actuator disk method in which the propeller is represented by some equivalent body force. The other is the full RANS approach in which the propeller is meshed geometrically.

The body force method in the study of self-propulsion is preferred because of considerably less computational time compared with the direct RANS simulation. One of the tricky elements in the body force method is the calculation of the induced velocity of the propeller, which is obtained from potential approaches. The effective wake of a ship as the result of the propeller's action is obtained by deducting induced velocity from total velocity.

In the body force method, Stern *et al*. (1988) first calculated and validated the body-propeller interactions of a DTNSRDC (David W. Taylor Naval Ship Research and Development Center) after the body model with propeller model 4577 via the partially parabolic method. The body force is either analytically prescribed through measured loads or obtained iteratively through the vortex lattice lifting surface method. The comparisons show that the computed results are in close agreement with experiment data available. Zhang *et al*. (1992) first studied the hull-propeller interaction of a ship (Series 60 model) using RANS and body force methods. The propeller body force was obtained by the lifting line theory. They compared the calculation of the velocity and pressure field with model test data by Toda; reasonable agreement was seen. Simonsen *et al*. (2005) coupled CFDSHIP-IOWA with a simplified potential theory based propeller code using the body force method. They computed the hull-propeller interaction of the Series 60 ship and then appended the tanker *Esso Osaka*. Comparisons between the calculated and the measured data show good agreement. Gao *et al*. (2010) carried out systematic study on body force parameters and mesh sensitivity of a container model and concluded that the grid density is more important than the model parameters for the study of hull-propeller interaction. More reference on the self-propulsion simulations using the body force method can be found in Tahara *et al*. (2006).

Direct RANS simulation in which the propeller and hull are geometrically meshed is relatively new and requires large computer resources. The advantage of the method is that there would be no uncertainties resulting from body force modelling, allowing induced velocity to be introduced. Abdel-Maksoud *et al*. (2000) computed hull-propeller interaction of Korean container ship (KCS) with the geometrically meshed propeller using Computational Fluid DynamiX (CFX). Although relatively coarse meshes were used, the numerical results were encouraging with error rates in the range of 5%−7% for predicted propeller loads.

Received date: 2011-11-15.
Foundation item: Supported by European Union FP7 program, ICT-231646, SHOAL: Search and monitoring of Harmful contaminants, Other pollutants And Leaks in vessels in port using a swarm of robotic fish.
***Corresponding author Email:** gao.q.x@strath.ac.uk

As a free surface was not taken into account in their calculations, total resistance cannot be therefore correctly predicted. Lübke (2005) studied the hull-propeller interaction of KCS with the geometrical modelling of a propeller using CFX. He investigated the mesh and time step effects on the hydrodynamic loads. Free surface elevation was prescribed from the potential based method. Overall, good agreement between the calculations and measurements was achieved. The results showed that the computed pressure resistance exhibits unrealistic high frequency oscillation, which would therefore introduce large errors in the simulation of self-propulsion. Carrica *et al*. (2010) adopted a Proportional-Integral (PI) speed controller to find the self-propulsion point of a free running ship using the overset grid technique of the latest code CFDSHIP-IOWA .

In this paper, the results of the full RANS simulation of ship self-propulsion are presented. The emphasis is on the induced velocity in the action of the rotating propeller. The induced velocity is then compared with that obtained via the RANS simulation of the propeller in open water tests and the momentum theory of the propeller. The structure of the paper is organised as follows: first, the mathematical and numerical formulations are described; then, the test cases of the ship and propeller, meshes, and computational procedures are presented; analysis and validation of the computed results follow. Finally, conclusions are drawn upon the practice of full RANS simulation of self-propulsion.

2 Numerical formulations

The RANS equations and RNG k-ε turbulence model are solved using the finite volume method (FVM). A VOF model is used to compute free surface elevation. The governing equations in the computational domain are as follows:

Continuity equation:

$$\nabla \cdot \boldsymbol{u} = 0 \tag{1}$$

Momentum equation:

$$\frac{\partial \boldsymbol{u}}{\partial t} + \boldsymbol{u} \cdot \nabla \boldsymbol{u} = -\frac{1}{\rho}\nabla p + \boldsymbol{g} + \nu \nabla^2 \boldsymbol{u} \tag{2}$$

Turbulence equations:

$$\frac{\partial}{\partial t}(\rho k) + \nabla \cdot (\rho \boldsymbol{u} k) = \nabla \cdot (\Gamma_k \nabla k) + G_k - Y_k \tag{3}$$

$$\frac{\partial}{\partial t}(\rho \varepsilon) + \nabla \cdot (\rho \boldsymbol{u} \varepsilon) = \nabla \cdot (\Gamma_\varepsilon \nabla \varepsilon) + G_\varepsilon - Y_\varepsilon \tag{4}$$

Volume fraction equation:

$$\frac{\partial}{\partial t}(r_w) + \nabla \cdot (r_w \boldsymbol{u}) = 0 \tag{5}$$

Second order upwind interpolation is used for the discretization of the convection flux. The SIMPLE method is applied to obtain velocity and pressure. Geometric reconstruction of the volume fraction is adopted to calculate wave elevation. References of theoretical and numerical aspects can be found in the ANSYS FLUENT user manual.

3 Test case

The test case uses simulation of self-propulsion on a container ship KCS with a bulbous bow, transom stern, and stern bulb. The propeller KP505 is a five-bladed fixed pitch propeller (FPP) model. The principle particulars of KCS and KP505 are in Table 1.

Table 1 Principle particles of ship and propeller

Ship model	KCS
Ship length L_{pp} / m	7.2786
Drought / m	0.3418
Wetted area / m^2	9.4379
Propeller model	5
Blade number / m^2	9.4379
Diameter / m	0.25
Hub ratio	0.18
Section profile	NACA 66 + a=0.8 camber line

The snapshot of geometry of test cases is given in Fig.1.

Fig.1 Geometries of ship and propeller

A total of around 7.9 million cells are generated for the calculation of self-propulsion. The propeller is meshed separately and the interface technique is adopted. About 3.0 million cells are used in the propeller block. A grid uncertainty study is carried out in separate calculations. Special care is given to the number of cells within a wave length in the wave amplitude and boundary layer. The meshes near the bow and stern are shown in Fig.2− Fig.3.

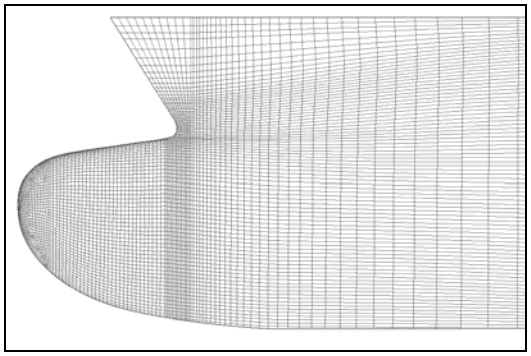

Fig.2 Meshes near the bow

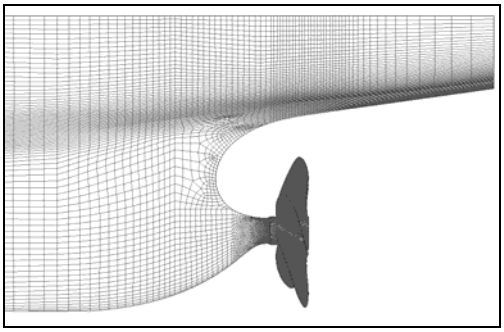

Fig.3 Meshes near the stern

The domain is shown in Fig.4. The inlet is located at one ship length in front of the bow where a uniform velocity of 2.1962 m/s and volume fraction is imposed. The outlet is at two ship lengths behind the stern where the hydrostatic pressure is specified. The revolution rate of the propeller is 9.5 rps.

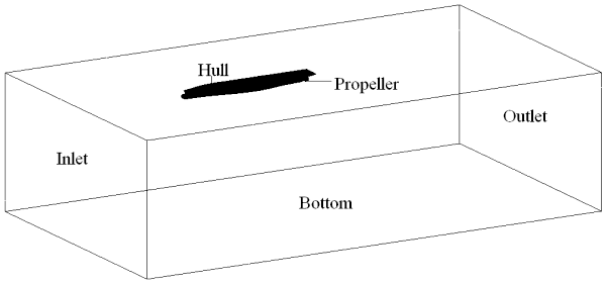

Fig.4 Computational domain

4 Numerical results

4.1 The validation of the self-propulsion results

The computed self-propulsion results at fixed rotational rate of 9.5 rps are compared with the measured data, and the computed velocity field is used to obtain the induced velocity of the propeller. The convergence histories of the total resistance on the hull and the thrust on the propeller are shown in Fig.5 and 6. With the rotation of the propeller, the thrust on the propeller depicts harmonic oscillations. The total resistance on the hull and the torque of the propeller show similar behaviour. Thrust and total resistance have the same phase angle. However, the amplitude of oscillation on the propeller is larger than that on the hull due to different effects of the flow field. The mean values are balanced with added towing force. The values of the forces and torque coefficients in Table 2 are time averaged.

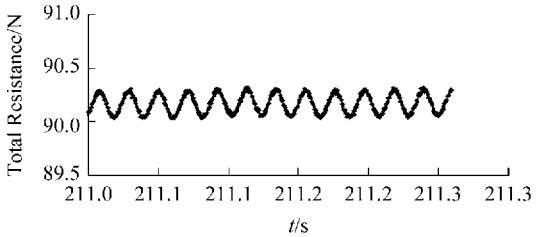

Fig.5 Total resistance convergence history

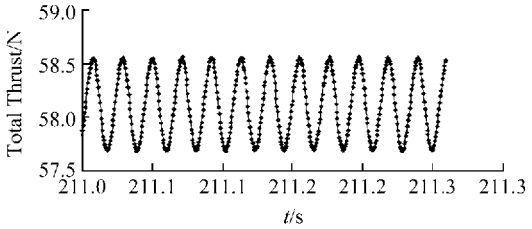

Fig.6 Total thrust convergence history

A comparison of the computed and measured propulsive factors is given in Table 2. It can be seen from the table that the computed resistance coefficients at the towing and self-propulsion conditions coincide well with EFD data. The thrust coefficient of the propeller is underestimated while the torque coefficient is slightly over the predicted level. The computed propulsive factors show good agreement with the experimental data.

Table 2 Comparison of propulsive factors

Factors	CFD	EFD	Error%
Bare hull resistance coefficient ($\times10^{-3}$)	3.510	3.550	−1.13
Propelled hull resistance coefficient ($\times10^{-3}$)	3.964	3.966	−0.05
Thrust coefficient K_T	0.165	0.170	−2.94
Torque coefficient $10K_Q$	0.290	0.288	+0.56
Thrust deduction factor $1-t$	0.852	0.853	−0.12
Taylor wake fraction $1-\omega_T$	0.772	0.792	−2.51
Advance coefficient J	0.714	0.728	−1.92
Propulsive efficiency η	0.715	0.740	−3.38

Comparisons of velocity contours at the section immediately behind the propeller plane (x/L_{pp}=0.9911) are shown in Fig.7−Fig.9. The velocity field changes with the rotation of the propeller. Thus, the results shown in these figures are time averaged over one cycle of the rotation. As can be seen from the velocity plots, the operation of the propeller changes the flow field significantly. The velocity contour is not symmetric about the central plane. The axial velocity increases remarkably in the propeller area due to acceleration effects. The maximum longitudinal velocity u/U is about 1.2 at the starboard side due to the clockwise rotation of the propeller. The flow is mixed as a result of the wake from the hull and that induced by the propeller, and eventually, axial velocity becomes more or less evenly distributed circumferentially around the propeller shaft. Although there is an acceptable qualitative agreement between the computed and the measured flow fields, discrepancies are observed near the axis of the propeller as shown in Fig.9. The computed results underestimate the acceleration of axial velocity and overestimate the rotational cross flow. The discrepancies may be attributed to the turbulence model used.

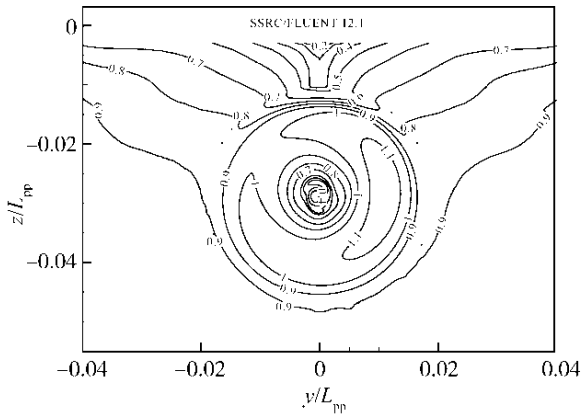

Fig.7 Computed axial velocity at x/L_{pp} =0.9911

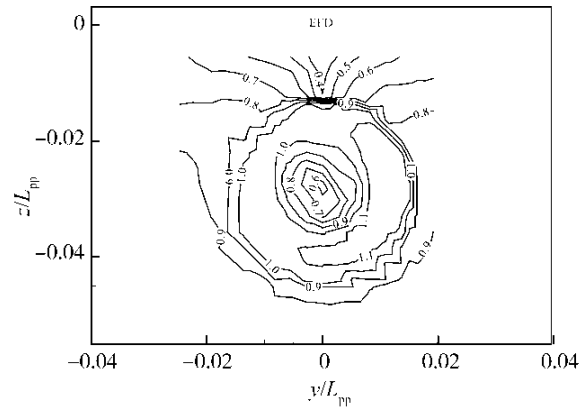

Fig.8 Measured axial velocity at x/L_{pp}=0.9911

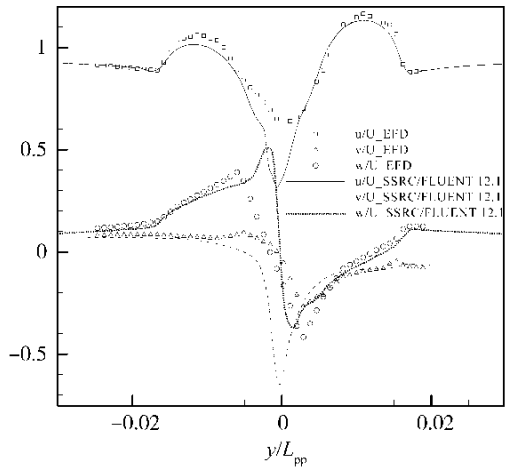

Fig.9 Comparison of velocity components (x/L_{pp}=0.9911, z/L_{pp}= −0.03)

4.2 The validation of the open water results

In order to validate the computed results, the open water characteristic performance of the propeller is calculated. The revolution rate of the propeller is the same as that in self-propulsion. The advance ratio J is adjusted by changing the advance speed. The single reference frame (SRF) method is used. Only one blade is meshed and computed due to the periodicity of the problem. The grid distribution in the open water simulation is the same as that in the simulation of self-propulsion. The computed results in Fig.10 indicate that the predicted torque coefficients are slightly overestimated while thrust coefficients are in good agreement with the data. Overall good agreement is achieved between the calculation and the experiment. It should be noted that the propulsive factors in Table 2 are computed based on the thrust identity method from the computed characteristic curve of the open water tests.

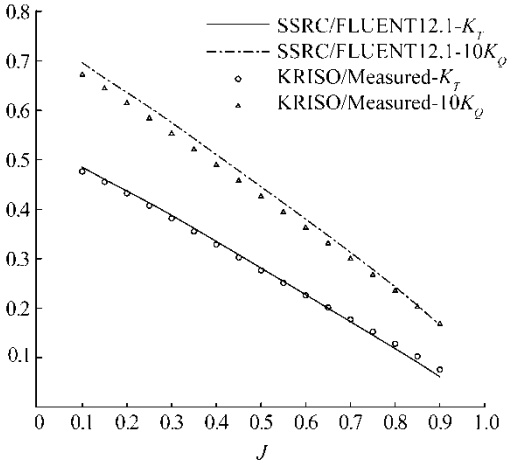

Fig.10 K_T and $10K_Q$ vs. J

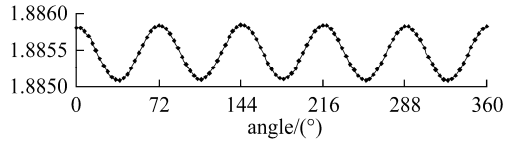

Fig.11 Total axial velocity on the propeller plane in one cycle

4.3 The comparison of propeller induced velocities

From the computed flow field, it can be found that propeller induced velocity varies periodically with the rotation of the propeller. Fig.11 presents the computed area averaged axial velocity at the propeller plane in one cycle of the rotation. The time averaged value is used to derive induced velocity. For open water calculation, the total axial velocity is time independent. The induced velocity from the momentum theory is also calculated and compared. The results are in Table 3.

Table 3 Comparison of computed induced velocities

Method	Computed induced velocity
Self-propulsion	$0.11V_A$
Open water	$0.10V_A$
Momentum theory	$0.18V_A$

As seen in Table 3, the induced velocities computed using RANS at self-propulsion and open water conditions coincide well. However, the induced velocity by the momentum theory is significantly overestimated, which will lead to a lower

effective wake with higher thrust and torque from the calculations of the propeller program.

5 Conclusions

RANS simulations of self-propulsion and open water tests using geometrical modelling of the propeller were carried out. Based on the numerical results, the following conclusions were drawn:

1) The computed velocity fields and the hydrodynamic coefficients were consistent with experimental data.

2) The induced velocities obtained by the RANS calculations agreed well; however, they were significantly overestimated by the momentum theory.

3) Although the results of RANS simulation using self-propulsion were encouraging, the computing time was significantly longer when compared with the body force method due to the increased grids and the moving mesh methods.

It is proposed that the RANS simulation of self-propulsion in free conditions could be considered in further works

References

Abdel-Maksoud M, Rieck K, Menter FR (2000). Unsteady numerical investigation of the turbulent flow around the container ship model (KCS) with and without propeller. *A Workshop on Numerical Ship Hydrodynamics*, Gothenburg.

Carrica PM, Castro AM, Stern F (2010). Self-propulsion computations using a speed controller and a discretized propeller with dynamic overset grids. *Journal of Marine Science and Technology*, **15**(4), 316-330.

Gao QX, Vassalos D (2010). The study of hull-propeller interaction by RANSE. *The 6th International Workshop on Ship Hydrodynamics*, Harbin.

Lübke LO (2005). Numerical simulation of the flow around the propelled KCS. *Proceedings of CFD Workshop Tokyo 2005*, Tokyo.

Simonsen CD, Stern F (2005). RANS maneuvering simulation of Esso Osaka with rudder and a body-force propeller. *Journal of Ship Research*, **49**(2), 98-120.

Stern F, Kim HT, Patel VC, Chen HC (1988). A viscous flow approach to the computation of propeller-hull interaction. *Journal of Ship Research*, **32**(4), 246-262.

Tahara Y, Wilson RV, Carrica PM, Stern F (2006). RANS simulation of a container ship using a single-phase level-set method with overset grids and the prognosis for extension to a self-propulsion simulator. *Journal of Marine Science and Technology*, **11**(4), 209-228.

Zhang DH, Broberg L, Larsson L, Dyne G (1992). A method for computing stern flows with an operating propeller. *Transactions of the Royal Institution of Naval Architects*, 245-259.

Qiuxin Gao B.Sc Peking University, 1985; M.Sc China Ship Scientific Research Centre, 1988; Ph.D University of Strathclyde; Currently researcher fellow in the Department of Naval Architecture and Marine Engineering, University of Strathclyde, specialised in computational fluid dynamics and experimental naval hydrodynamics; working on EU funded research projects, VIRTUE, SHOAL, TARGET.

Wei Jin B.Sc Wuhan University of Science and Technology, 2006; M.Sc Shanghai JiaoTong University, 2009; Currently PhD candidate in the Department of Naval Architecture and Marine Engineering, University of Strathclyde. Skilled in computational fluid hydrodynamic, working on engine combustion, heat transfer, and ship propulsion.

Dracos Vassalos Currently Professor in the Department of Naval Architecture and Marine Engineering, University of Strathclyde, 30 years research, development and application on the stability of ships and advanced marine vehicles; technical Programme Committee of ISOPE since 1991, member of the Editorial Board: Journal of "Marine Science and Technology"; Journal of "Maritime Research"; Journal of "Marine Systems and Ocean Technology"; EU Editor in Chief of the Journal of "Ships and Offshore Structures";